Journal of Electrical Engineering, Vol. 74, No. 6, 2023, pp. 474-484

sciendo

PAPERS

A comparative study on real-time sitting posture monitoring systems using pressure sensors

Liang Zhao[1], Jingyu Yan[2], Aiguo Wang[2*]

Accurate sitting posture recognition plays a crucial role in improving improper postures and reducing the risk of associated health issues. The inherent complexity of human behavior, however, poses a great challenge to the development of a practical sitting posture monitoring system with pressure sensors. Towards facilitating the use of features, choice of classification models, and way of evaluating a sitting posture recognizer, in this study a comparative study on pressure-sensor-based sitting posture monitoring is conducted. Specifically, we extract discriminant features from the sensor data based on the distribution of pressure sensors and explore different combinations of these features. Then, five commonly used classification models are evaluated towards building a robust sitting posture recognizer. Finally, extensive comparative experiments concerning four performance metrics are conducted on the collected datasets in *subject-dependent*, *subject-independent*, and *cross-subject* settings. Results show that the joint use of sensors at different positions leads to higher accuracy and that random forest generally outperforms the other four classification models. Surprisingly, compared to the *subject-dependent* and *subject-independent* settings, *cross-subject* setting greatly suffers from degraded accuracy, where we preliminarily present the results of transfer learning techniques to mitigate this issue. In addition, we perform parameter sensitivity and time-cost analysis of random forest, which indicates its applicability to practical use.

Keywords: sitting posture monitoring, pressure sensor, subject-independent, subject-dependent, cross-subject

1 Introduction

With the advancement of technology and specialization of social roles, prolonged sedentary behavior has nowadays become a prevalent lifestyle and working condition, and consequently the associated health implications have gained widespread attention and concerns in society, particularly for the well-being of adolescents. Extensive researches have shown that a strong correlation exists between poor sitting postures and musculoskeletal disorders (e.g., cervical spondylosis, chronic back pain, improper spinal alignment, joint and muscle discomfort, and intervertebral disc injuries). Even worse, poor sitting postures can lead to higher risks of diseases and mortality and even psychological diseases such as fatigue and depression [1].

Studies on sitting posture monitoring not only help reduce the health hazards linked to prolonged sitting and improve sitting habits, but also capture sitting posture data for assisting medical professionals in analyzing the underlying causes of certain diseases and making effective treatment plans [2]. Accordingly, researchers have conducted a large number of studies [3,4]. For example, Taieb-Maimon et al. facilitated the timely adjustment of poor sitting postures by comparing the sensed sitting posture images with that of proper sitting postures, and this study shows an improvement in the sitting habits of participants [5]. As a pervasive computing technology, sitting posture monitoring has also been applied in various domains. For example, in the realm of human-computer interaction, game interfaces dynamically adjust the movements and positions of players towards more immersive and realistic gaming experiences. Smart home systems adapt lighting and temperature along with the sitting postures, facilitating a comfortable living environment. Due to the variations arising from work environments and user sitting habits, however, sitting postures exhibit unique characteristics such as diversity, occurrence, similarity, and inter-subject variability. For example, one probably performs the same sitting posture differently at different times and locations (i.e., intra-subject variation), different individuals would perform the same sitting posture differently (i.e., inter-subject variation), and different sitting postures may trigger similar sensor readings (i.e., similarity between different sitting postures). Hence, sitting posture monitoring is a challenging yet meaningful topic [6].

According to the used sensors, existing sitting posture recognition methods can be broadly categorized into four groups: vision-based, wearable sensor-based, environment sensor-based, and pressure sensor-based methods. Vision-based methods use computer vision techniques to capture real-time depth images and to recognize sitting postures [7]. Clearly, such methods often raise concerns regarding privacy and are sensitive to variations in lighting conditions and occlusions.

[1] School of Computer and Information Engineering, Chuzhou University, Chuzhou, China
[2] School of Electronic Information Engineering, Foshan University, Foshan, China
* wangaiguo2546@163.com

https://doi.org/10.2478/jee-2023-0055, Print (till 2015) ISSN 1335-3632, On-line ISSN 1339-309X

Wearable sensor-based methods collect posture data using sensors worn on human body parts (e.g., the back, neck, and legs) and then train a sitting posture recognizer [8]. Commonly used sensing units include, but not limited to, accelerometers, gyroscopes, strain sensors, and among others. For instance, Qian et al. utilized the strain gauge attached to one's back to acquire sitting data and trained a three-layer neural network to classify normal sitting posture, slight kyphosis, and severe kyphosis [9]. The long-term use of wearable sensors, though convenient, would greatly impact user experience. In contrast, environment sensor-based methods utilize mediums such as WiFi, millimeter waves, and infrared sensors to sense and recognize postures. For example, Feng et al. used three RFID tags to investigate the correlation between RFID tag phase shifts and sitting postures and then used it to infer upright posture, forward-leaning, and tilt back [10]. Such methods are less/non-invasive, but vulnerable to environmental factors such as temperature, humidity, and lighting.

Compared to the above methods, the utilization of pressure sensors offers advantages such as affordability and better user privacy. Specifically, sitting posture monitoring with pressure sensors captures the pressure distribution of different sitting postures and then builds a model to recognize sitting postures. For example, Hu et al. developed a sensing unit consisting of six flexible pressure sensors and employed a sliding window to extract features from the seat cushion, backrest, and armrest. A two-layer artificial neural network was trained to recognize seven sitting postures. They get 97.78% accuracy with floating-point calculation and 97.43% with fixed-point calculation [11]. Anwary et al. designed a seat cover embedded with pressure sensors and built a rule-based model by comparing the sensor readings of the left side and right side to infer the duration of asymmetric sitting postures [12]. Bourahmoune et al. proposed a posture and stretching recognition system with a pressure cushion and machine learning model [13]. Roh et al. developed a posture monitoring system with four weighing sensors placed beneath the chair to infer six different sitting postures with features extracted from the sensor data and the user's body weights [14]. Jeong et al. embedded six pressure sensors in the seat cushion to collect pressure data and placed six infrared reflective distance sensors in the chair backrest to measure the distance between the backrest and user's torso. *k*-nearest neighbor was used to predict 11 distinct postures [15].

While progresses have been made in pressure sensor-based sitting posture monitoring, there are aspects needing further studies [16-18]. First, feature engineering and classification models are important factors largely determining the recognition performance, however, few studies have systematically evaluated the use of features extracted from pressure sensor data and the choice of classifiers. Second, most of existing studies, to the best of our knowledge, evaluate the performance of sitting posture recognizers in the subject-independent setting, which may over-estimate their abilities. To this end, we herein conduct a comparative study on sitting posture monitoring with pressure sensors. The main contributions of our study are as follows.

(1) Discriminant features are extracted based on the distribution of pressure sensors and their relationships with different sitting postures. Specifically, we extract features from data of the seat pan sensors, backrest sensor, and center of pressure distribution. We also evaluate the power of these features when they are used separately and jointly.

(2) Three different evaluation settings, i.e., subject-dependent, subject-independent, and cross-subject, are considered towards better analyzing a sitting posture recognizer. This reminds us of the distribution difference of sensor data between users.

(3) Extensive comparative experiments on five classification models (i.e., *k*-nearest neighbors, naive Bayes, decision trees, XGBoost, and random forest) concerning four performance metrics are conducted. Results show that random forest generally outperforms its competitors and that a recognizer in the cross-subject setting often suffers from degraded accuracy, where we show transfer learning is a potential tool. Besides, parameter sensitivity and time-cost analyses are conducted towards the tradeoff between accuracy and energy consumption.

2 The proposed sitting posture monitoring system

2.1 Sitting posture recognition framework

Figure 1 presents the sitting posture recognition framework, which consists of a training phase and a prediction phase. The training stage segments the collected sensor data using a sliding window and then extracts discriminant features from each segment to return a feature vector. Finally, a sitting posture recognizer *cls* is trained on the feature vectors. During the prediction phase, the streaming sensor data are collected with posture sensing units. Afterwards, the feature extraction corresponding to the training phase is utilized to obtain feature vectors, which are then sent to the *cls* for recognizing sitting postures.

The posture sensing unit in our study mainly consists of three modules: data acquisition module, data processing module, and data uploading module [6]. The data acquisition module consists of five pressure sensors: four sensors placed at the four corners of the seat pan (S_1, S_2, S_3, and S_4 in Fig. 1) and one sensor on the backrest (S_5 in Fig. 1). Their working frequency is set at 400 Hz. The data processing module is equipped with

a stm32f103c8t6 processor and uses the arithmetic mean filtering to smooth the raw sensor readings every 20 sampled data points. The data uploading module transmits the sensed data to remote servers for subsequent analysis and processing.

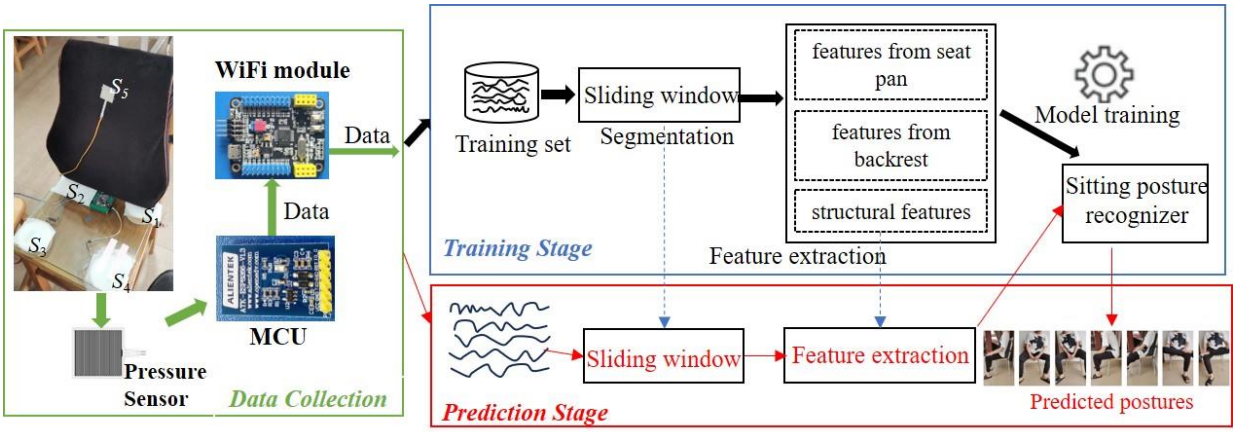

Fig. 1. Sitting posture recognition framework

2.2 Feature extraction

We in this study extract the discriminant features based on the distribution of pressure sensors and their relationships with different sitting postures.

Features extracted from the backrest sensor data. The backrest sensor can be used to infer whether one leans against the chair. We here only use time-domain features: mean, variance, maximum, and minimum, and denote them as F_b.

Features extracted from the seat pan sensor data. For time-domain features, mean, variance, standard deviation, maximum, minimum, zero-crossing rate, mode, and difference between the maximum and minimum are extracted. For frequency-domain features, we first use fast Fourier transform to obtain frequency-domain signals. Afterwards, we empirically extract DC component, mean, variance, standard deviation, slope, and kurtosis from both the frequency spectrum and amplitude. For simplicity, we note these features as F_s.

Besides, considering the relationship between sitting postures and gravity center, we also extract the structural feature, which uses formula (1) to get the gravity coordinates (x, y)

$$\begin{cases} x = L * \dfrac{V_2 + V_3}{\sum_{i=1}^{4} V_i} - \dfrac{L}{2} \\ y = W * \dfrac{V_3 + V_4}{\sum_{i=1}^{4} V_i} - \dfrac{W}{2} \end{cases} \quad (1)$$

where L and W are the length and width of the seat pan, respectively, and V_i is the reading of sensor S_i $(1 \le i \le 4)$. To reflect the variation of gravity coordinates, we extract time-domain features: mean, variance, maximum, and minimum, and denote them as F_g.

3 Experimental setup and results

3.1 Data collection

In the experiments, four participants are provided with chairs equipped with pressure sensors. The placements of pressure sensors are shown in Fig. 1. The participants are four males aged between 24 and 25, with weights between 60 and 68 kg and heights between 170 and 175 cm. Table 1 gives basic information of the participants.

To capture sitting posture data in a natural and uncontrolled way, volunteers are asked to perform seven predefined sitting postures, including upright (correct sitting posture), leaning left, leaning right, leaning forward, leaning backward, right leg crossed, and left leg crossed, in their own style (that is, they are not provided illustrations of sitting postures to be performed), during which, the system collects the sensor signals. Each sample contains the values of pressure sensors. Fig. 2 illustrates the sitting postures.

Table 1. Basic information on the volunteers

Volunteer ID	Gender	Age	Height/cm	Weight/kg
id1	Male	25	170	64
id2	Male	24	171	60
id3	Male	25	173	68
id4	Male	25	175	68

(a) (b) (c) (d) (e) (f) (g)

Fig. 2. Illustration of different sitting postures: (a) upright, (b) leaning left, (c) leaning right, (d) leaning forward, (e) leaning backward, (f) right leg crossed, (g) left leg crossed

Particularly, to annotate the streaming sensor data without compromising user experience, we position a camera in front of the volunteer to record the experimental process and use it to annotate sensor readings by replaying the videos. In this experiment, we collected sensor data with a duration of 12 minutes for each volunteer.

3.2 Experimental setup

For the streaming pressure sensor data, we employ a sliding window with 1s size to segment data and extract discriminant features from each segment. Afterwards, we use them separately or jointly to train a sitting posture recognizer. Herein, we consider the use of F_s, F_g, F_s & F_g, F_b, and F_s & F_g & F_b.

For the choice of classification models, five commonly used ones, including K-nearest neighbors with k=1 (KNN), naive Bayes (NB), decision tree (DT), XGBoost, and random forest (RF), are evaluated [19]. Accuracy (*acc*), precision (*pre*), recall (*rec*), and $F1$ are used as the performance metrics. Specifically, given $L=\{L_1, L_2, \ldots, L_{|L|}\}$ representing a set of labels with $|L|$ classes,

$$accuracy = \sum_{i=1}^{|L|} \frac{Num_i}{N} \tag{2}$$

where N represents the total number of samples, Num_i denotes the number of samples from class L_i that are correctly classified.

$$precision = \frac{1}{|L|} \sum_{i=1}^{|L|} \frac{Num_i}{NP_i} \tag{3}$$

$$recall = \frac{1}{|L|} \sum_{i=1}^{|L|} \frac{Num_i}{NT_i} \tag{4}$$

Here, NP_i represents the number of samples predicted as class L_i, and NT_i indicates the number of samples from class L_i.

$$F1 = \frac{2 \times precision \times recall}{precision + recall} \tag{5}$$

Besides, we consider three evaluation settings, i.e., subject-dependent, subject-independent, and cross-subject, for better analyzing the generalization ability of a sitting posture recognizer. Subject-dependent setting trains the sitting posture recognizer with the training set of a specific individual and tests it on the test set of the same individual. Subject-independent setting optimizes the sitting posture recognizer using the training data of all individuals and tests it on test data from all individuals. Cross-subject setting trains the sitting posture recognizer on the data of individual A and evaluates its performance on the data of individual B.

3.3 Results of subject-independent setting

In this setting, we combine sensor data of all participants and then utilize a stratified ten-fold cross-validation to generate independent training and testing sets, where each fold is used as a testing set and the remaining nine folds serve as training set. We train a posture recognizer on the training set and evaluate its performance on the testing set. The final experimental results are the average of the ten iterations. Table 2 presents the accuracy, where the best results for each classification model and each feature set are shown in bold and underlined, respectively. For better illustration, we also present the results in Fig. 3. From Tab. 2 we can observe that the joint use of different feature sets generally obtains higher accuracy except KNN. This is possibly because there exist redundant features. For example, RF achieves the highest accuracy of 95.45% on F_s & F_g & F_b, which is higher than that of F_s (94.10%), F_g (90.04), F_s & F_g (94.43), and F_b (46.11%). Not surprisingly, the single use of F_b obtains the lowest accuracy. Second, from the view of classifiers, we can see that RF generally gets better performance. For instance, it obtains 95.45% accuracy, which is comparable to XGBoost (95.64%) and outperforms KNN (75.51%), 65.33% (NB) and 91.28% (DT). Similar observations can also be seen in Fig. 4.

Table 2. Accuracy of subject-independent experiments

Features	KNN	NB	DT	XGBoost	RF
F_s	75.51	64.02	90.21	94.08	<u>94.10</u>
F_g	**88.92**	64.24	86.67	89.22	<u>90.04</u>
F_s & F_g	75.51	64.02	90.26	94.13	<u>94.43</u>
F_b	39.77	33.71	41.94	<u>48.97</u>	46.11
F_s & F_g & F_b	75.51	**65.33**	**91.28**	**<u>95.64</u>**	**95.45**

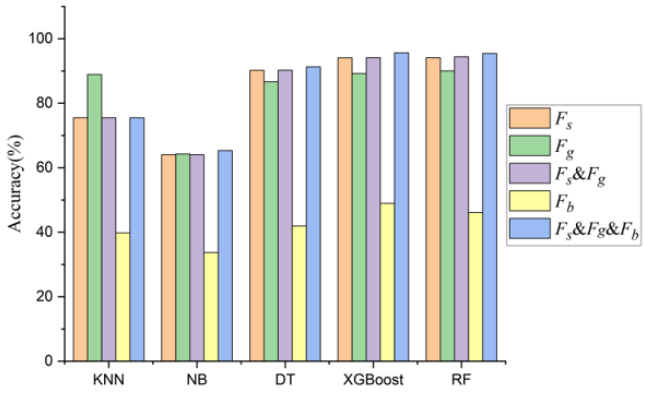

Fig. 3. Accuracy of subject-independent experiments

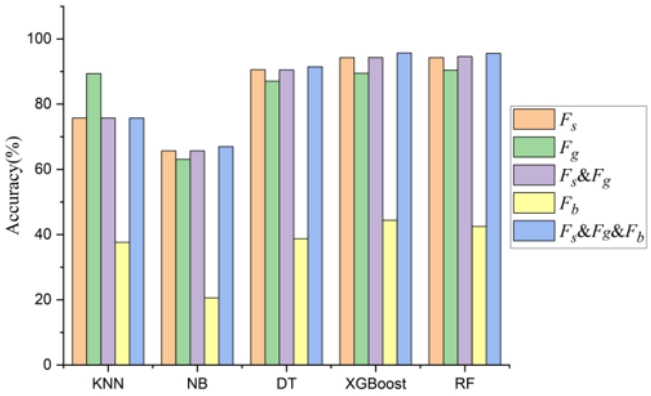

Fig. 4. $F1$ of subject-independent experiments

To facilitate a deep analysis of misclassifications among different sitting postures, Fig. 5 gives confusion matrices of RF for different feature sets, where 0 to 6 correspond to upright, leaning left, leaning right, leaning forward, leaning backward, left leg crossed, and right leg crossed. From Fig. 5, we can observe that the use of F_b enhances the differentiation between leaning forward and upright. For instance, 13 leaning forward samples are misclassified as upright without F_b and 10 leaning forward samples are misclassified as upright with F_b.

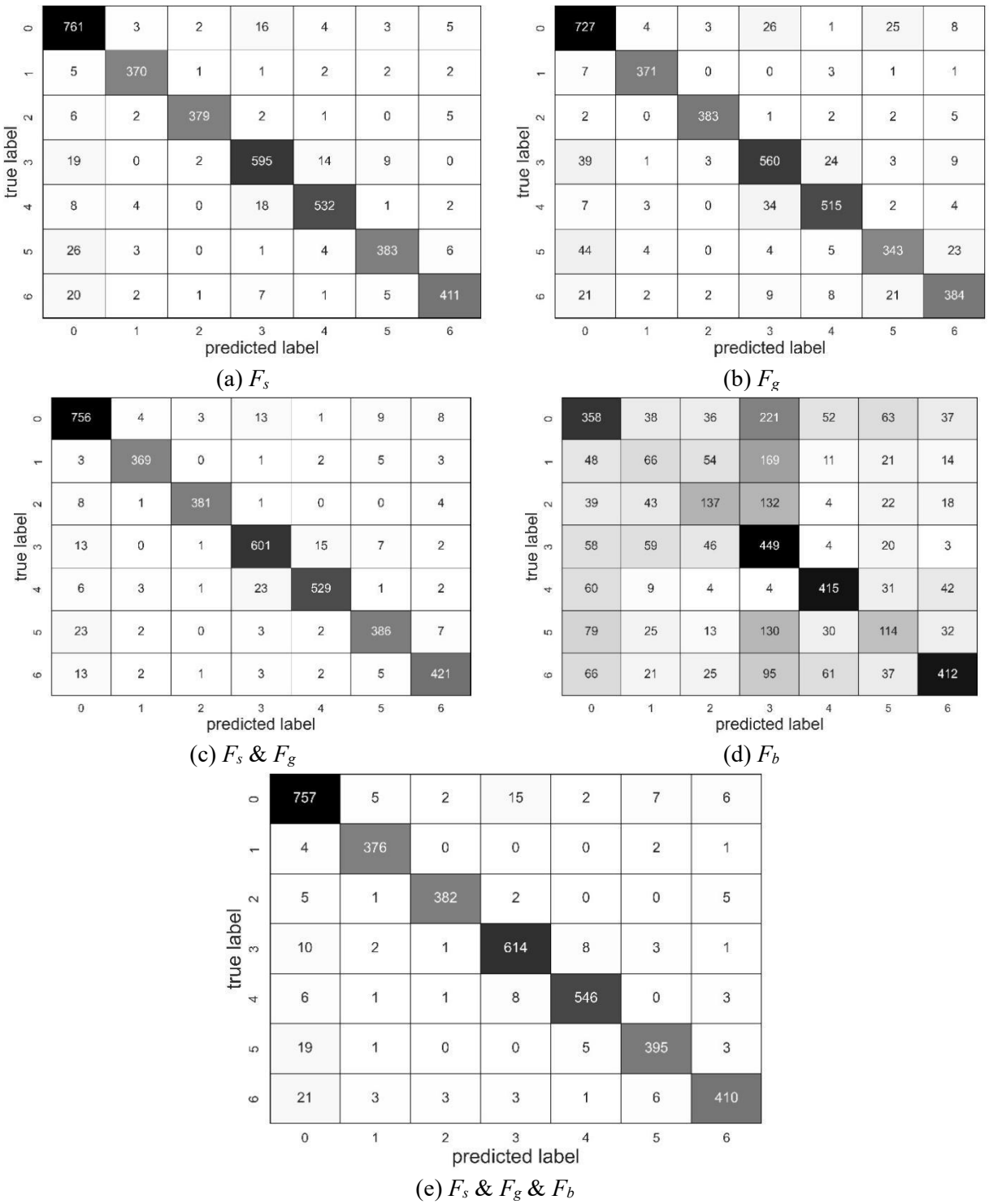

Fig. 5. Confusion matrices of subject-independent experiments. (a) F_s, (b) F_g, (c) F_s & F_g, (d) F_b, (e) F_s & F_g & F_b

3.4 Results of subject-dependent setting

A stratified ten-fold cross-validation is employed to generate independent training and testing sets, where each fold is used as a testing set while the remaining nine folds serve as the training set. We train the sitting posture recognition model on the training set and evaluate its power on the testing set. The final results are the average of ten results. Table 3 shows the results, where the best accuracy for each classification model is shown in bold. From Tab. 3, we can observe that RF generally gets comparable performance to XGBoost and outperforms KNN, NB, and DT. For example, for id1, RF achieves accuracy of 98.09% on *Fs* & F_g & F_b, while KNN, NB, DT, and XGBoost get accuracy of 82.93%, 82.33%, 96.18%, and 97.37%, respectively. Second, the use of F_g

for KNN remains a priority and the joint use of different features fails to consistently get better accuracy. This is due to redundant features.

3.5 Results of cross-subject setting

Table 4 presents the cross-subject results with F_s & F_g & F_b, where "A => B" denotes that data from user A is used to train a sitting posture recognizer and data from user B is used to test its accuracy. We can see a notable decline in accuracy compared with subject-dependent and subject-independent settings. For example, RF only gets 46.29% accuracy for id1 => id2, compared to the 95.45% of subject-independent case and 98.09% of subject-dependent case.

This is mainly because of the difference between distributions of training and testing sets. One feasible solution is to utilize transfer learning to generalize knowledge from source to target domain [20]. Table 5 shows the preliminary results of three transfer learning algorithms (i.e., Stratified Transfer Learning (STL), Balanced Distribution Adaptation (BDA), and easy Transfer Learning). We see that transfer learning helps obtain enhanced accuracy.

Table 3. Results of subject-dependent experiments

Features		KNN		NB		DT		XGBoost		RF	
		Acc	*F*1	*Acc*	*F*1	*Acc*	*F*1	*Acc*	*F*1	*Acc*	*F*1
id1	F_s	82.93	82.59	78.63	80.38	94.63	95.04	95.94	96.17	96.87	96.89
	F_g	**94.27**	94.82	75.53	78.02	92.84	93.36	97.25	97.21	97.85	95.78
	F_s & F_g	82.93	82.59	78.63	80.38	94.15	94.70	96.30	96.52	96.78	96.98
	F_b	63.96	60.67	60.73	51.73	69.22	66.40	73.75	70.44	71.96	68.00
	F_s & F_g & F_b	82.93	82.59	**82.33**	84.10	**96.18**	96.28	**97.37**	97.43	**98.09**	98.12
id2	F_s	**94.95**	95.26	94.95	95.06	86.36	86.46	96.02	96.40	96.24	96.46
	F_g	93.66	93.54	81.20	80.64	91.40	91.42	93.34	93.39	93.45	93.23
	F_s & F_g	86.36	86.46	**95.06**	95.32	**94.95**	95.34	**96.35**	96.55	96.67	96.88
	F_b	33.84	27.32	27.93	23.64	35.34	28.06	36.41	27.60	35.88	28.68
	F_s & F_g & F_b	86.36	86.46	**95.06**	95.33	94.84	95.02	**96.35**	96.51	**96.78**	97.01
id3	F_s	75.13	74.22	83.42	79.15	94.82	94.52	97.10	97.05	96.37	96.42
	F_g	**93.67**	93.60	82.79	82.87	92.84	92.75	93.57	93.70	92.94	93.41
	F_s & F_g	82.01	75.57	83.42	79.66	95.44	95.07	96.37	96.33	96.47	96.51
	F_b	60.41	58.55	57.72	48.77	64.77	61.10	69.22	65.17	67.25	64.33
	F_s & F_g & F_b	75.13	74.22	**83.62**	79.30	**95.75**	95.58	**97.72**	97.57	**97.61**	97.46
id4	F_s	67.62	62.11	**86.06**	84.06	87.60	85.16	93.09	91.66	92.21	90.96
	F_g	**89.24**	87.39	82.44	81.88	**89.02**	86.97	91.44	90.16	91.00	89.67
	F_s & F_g	67.62	62.11	**86.06**	84.06	88.04	86.53	93.64	92.82	92.82	92.93
	F_b	46.43	36.35	21.96	19.18	46.87	36.12	50.17	37.99	47.86	35.99
	F_s & F_g & F_b	67.18	61.69	85.62	84.49	88.59	86.70	**94.19**	93.19	**93.20**	92.00

Table 4. Results of cross-subject experiments

	KNN		NB		DT		XGBoost		RF	
	Acc	*F*1	*Acc*	*F*1	*Acc*	*F*1	*Acc*	*F*1	*Acc*	*F*1
id1 => id2	50.59	51.77	49.09	42.44	14.29	9.06	42.00	30.53	46.29	39.87
id2 => id1	35.32	25.10	52.15	47.10	33.53	20.06	20.88	9.72	34.61	27.59
id1 => id3	21.04	24.68	30.78	25.81	31.19	25.44	51.50	42.20	24.56	25.09
id3 => id1	10.50	15.03	28.64	20.33	34.13	24.74	17.90	19.93	37.95	28.84
id1 => id4	32.27	29.98	34.69	31.37	32.27	26.4	40.07	39.41	39.41	37.47
id4 => id1	20.88	23.03	48.21	43.68	45.11	41.61	50.84	45.22	45.94	43.72
id2 => id3	28.29	30.38	30.36	33.18	40.00	35.39	26.94	25.56	45.08	44.89
id3 => id2	27.6	33.06	28.03	31.55	21.37	14.51	27.07	29.71	48.76	42.26
id2 => id4	31.17	36.56	17.78	17.80	17.19	15.59	30.08	28.49	34.47	35.27
id4 => id2	29.97	25.35	39.74	34.55	30.40	22.38	66.70	59.83	60.69	49.27
id3 => id4	18.22	20.95	49.4	32.05	29.64	24.96	49.62	38.71	51.48	47.38
id4 => id3	22.18	26.62	47.25	40.55	44.66	34.75	65.49	57.98	34.2	35.42

Table 5. Preliminary results of transfer learning experiments

Transfer Learning	STL		BDA		easyTL	
	Acc	*F*1	*Acc*	*F*1	*Acc*	*F*1
id1 => id2	43.72	40.19	48.43	40.75	57.46	47.69
id2 => id1	26.01	32.45	42.17	36.70	37.71	27.26
id1 => id3	38.76	40.21	36.20	33.47	30.47	25.85
id3 => id1	41.41	40.32	26.16	24.68	29.48	33.44
id1 => id4	62.02	50.04	43.53	42.52	44.45	46.66
id4 => id1	44.63	45.84	44.27	43.05	38.90	33.59
id2 => id3	51.40	52.95	41.09	35.08	39.59	34.86
id3 => id2	59.94	54.38	44.38	38.18	60.15	53.81
id2 => id4	50.27	50.13	40.34	38.94	31.28	27.95
id4 => id2	44.15	42.56	58.07	56.61	38.89	31.73
id3 => id4	43.69	45.97	37.06	35.07	44.13	43.48
id4 => id3	33.47	35.76	51.50	50.14	51.50	44.47

3.6 Evaluation of the size of sliding window

We assess the influence of sliding window size on the performance of RF-based recognizer. Fig. 6 presents the results, where the X-axis represents sliding window size and Y-axis is the accuracy. The candidate values are 1, 3, and 5s. Fig. 6(a) shows the subject-dependent accuracy. It can be seen that accuracy decreases with the increase of window size except the use of F_b. Fig. 6(b) shows the subject-independent accuracy on id1. We can observe that the accuracy decreases with the increase of window size. Fig. 6(c) presents the cross-subject accuracy where the training data is from id1 and test data is from id4.

3.7 Evaluation of the number of trees

Considering the superiority of RF, we further evaluate the number of trees on the recognition accuracy. The candidate values are 10, 25, and 50. Figure 7 presents the accuracy for both the subject-independent case and subject-dependent case. From Fig. 7, we can observe that the accuracy of RF is less sensitive to the number of trees.

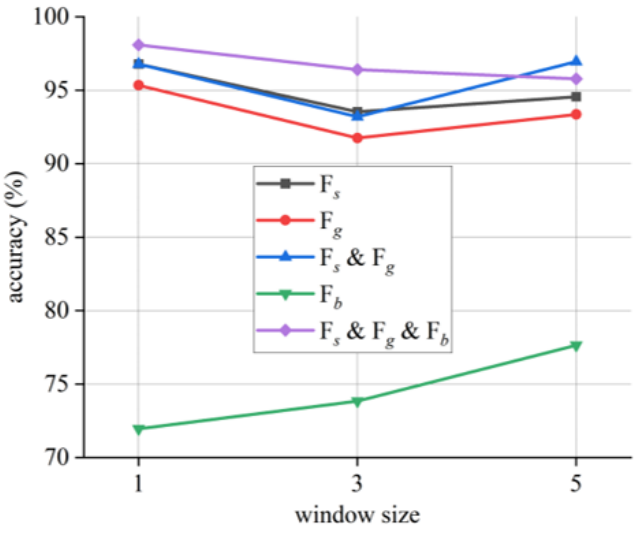

(a) subject-dependent setting

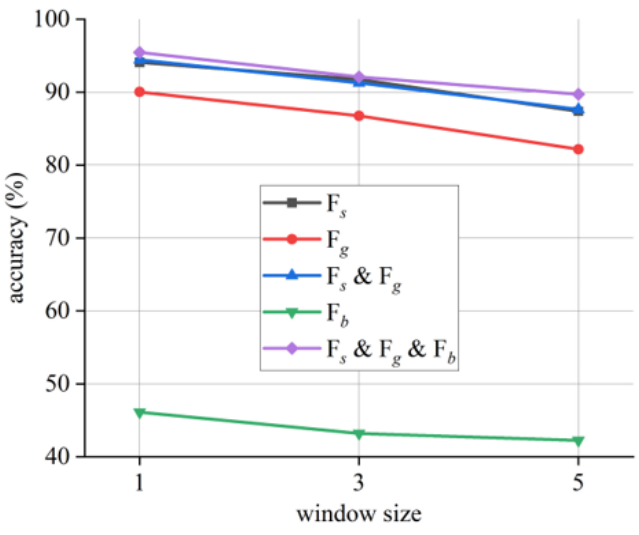

(b) subject-independent setting

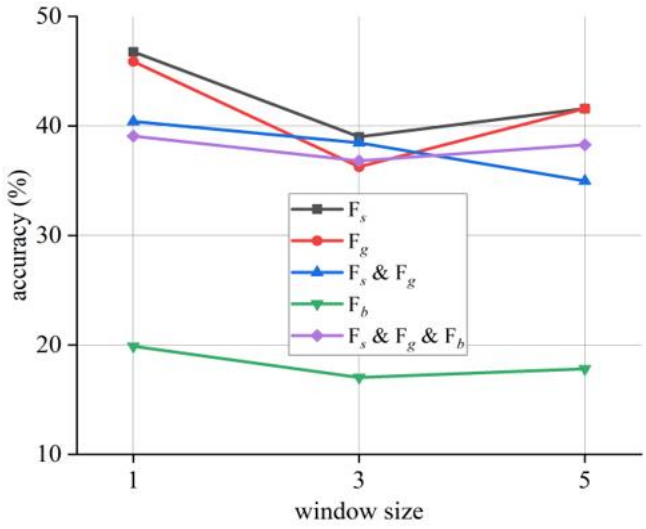

(c) cross-subject setting

Fig. 6. Parameter sensitivity analysis: (a) subject-dependent setting, (b) subject-independent setting, (c) cross-subject setting

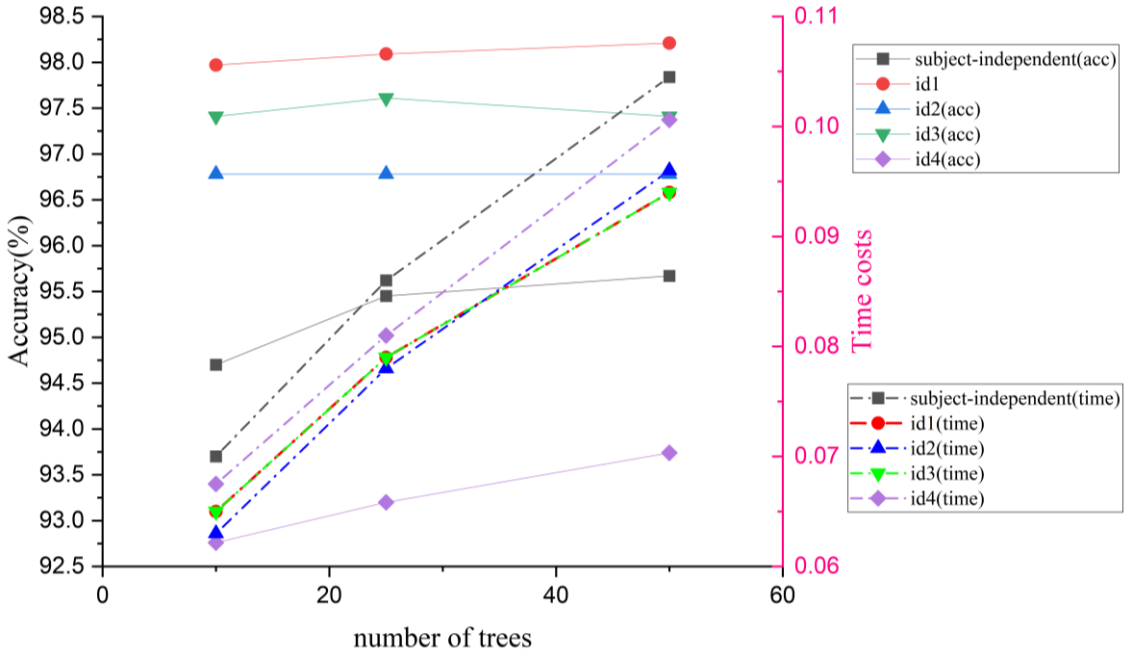

Fig. 7. Accuracy and time cost *versus* the number of trees

3.8 Time cost

Besides accuracy, time cost is an important factor for sitting posture recognition systems. We herein present the time cost of RF-based recognizer and conduct experiments on a computer with a core i5-12490f CPU and 32G RAM. Fig. 7 gives the time cost (in seconds) versus the number of trees, where we can see that RF can satisfy real-time processing requirement and that the use of 25 achieves a better tradeoff between accuracy and time consumption.

4 Conclusions

A comparative study on sitting posture recognition using pressure sensors is conducted in this study. We extract different discriminant features based on the distribution of pressure sensors and their relationships with different sitting postures and then evaluate their power. Then, five commonly used classification models (i.e., KNN, NB, DT, XGBoost, and RF) are considered. Finally, we conduct comparative experiments concerning four performance metrics in three different settings (*ie* subject-dependent, subject-independent, and

cross-subject). Results indicate that random forest generally remains a priority and that cross-subject sitting posture recognizers often suffer from lower accuracy, where we preliminarily show the potential use of transfer learning to this issue.

For future work, this study only initially highlights the significance of cross-subject sitting posture recognition, and hence how to utilize transfer learning techniques to mitigate this issue deserves further study.

Acknowledgments

This work was supported by the Natural Science Research of the Anhui Higher Education Institution (Nos. KJ2020A0725, KJ2021ZD0127).

References

[1] J. Withall, A. Stathi, M. Davis, J. Coulson, J. L. Thompson, and K. R. Fox, "Objective indicators of physical activity and sedentary time and associations with subjective well-being in adults aged 70 and over," *International Journal of Environmental Research and Public Health*, vol. 11, no. 1, pp. 643-656, 2014, doi:10.3390/ijerph110100643

[2] M.-C. Tsai, E. Chu, and C. R, Lee, "An automated sitting posture recognition system utilizing pressure sensors," *Sensors*, vol. 23, no. 13, pp. 5894, 2023, doi:10.3390/s23135894

[3] I. Wijegunawardana, R. Ranaweera, and R. Gopura, "Lower extremity posture assistive wearable devices: A review," *IEEE Transactions on Human-Machine Systems*, vol. 53, no.1, pp. 98-112, 2023, doi:10.1109/THMS.2022.3216761

[4] A. Kulikajevas, R. Maskeliunas, and R. Damaševičius, "Detection of sitting posture using hierarchical image composition and deep learning," *PeerJ Computer Science*, vol. 7, pp. e442, 2021, doi:10.7717/peerj-cs.442

[5] M. Taieb-Maimon, J. Cwikel, B. Shapira, and I. Orenstein, "The effectiveness of a training method using self-modeling webcam photos for reducing musculoskeletal risk among office workers using computers," *Applied Ergon*, vol. 43, no. 2, pp. 376-385, 2021, doi:10.1016/j.apergo.2011.05.015

[6] J. Yan, and A. Wang, "iGuard: An intelligent sitting posture monitoring system with pressure sensors," *2023 Third International Conference on Computer Vision and Pattern Analysis (ICCPA)*, 2023

[7] L. Li, G. Yang, Y. Li, D. Zhu, and L. He, "Abnormal sitting posture recognition based on multi-scale spatiotemporal features of skeleton graph," *Engineering Applications of Artificial Intelligence*, vol. 123, pp. 106374, 2023, doi:10.1016/j.engappai.2023.106374

[8] S. Ma, W. H. Cho, C. H. Quan, and S. Lee, "A sitting posture recognition system based on 3-axis accelerometer," *2016 IEEE Conference on Computational Intelligence in Bioinformatics and Computational Biology (CIBCB)*, 2016, doi:10.1109/CIBCB.2016.7758131

[9] Z. Qian, A. Bowden, D. Zhang, J. Wan, W. Liu, X. Li, D. Baradoy, and D. T. Fullwood, "Inverse piezoresistive nanocomposite sensors for identifying human sitting posture," *Sensors*, vol. 18, no. 6, pp. 1745, 2018, doi: 10.3390/s18061745

[10] L. Feng, Z. Li, and C. Liu, "Are you sitting right? Sitting posture recognition using RF signals", *2019 IEEE Pacific Rim Conference on Communications, Computers and Signal Processing (PACRIM)*, 2019, doi:10.1109/PACRIM47961.2019.8985070

[11] Q. Hu, X. Tang, and W. Tang, "A smart chair sitting posture recognition system using flex sensors and FPGA implemented artificial neural network," *IEEE Sensors Journal*, vol. 20, no. 14, pp. 8007-8016, 2020, doi:10.1109/JSEN.2020.2980207

[12] A. Anwarya, D. Cetinkaya, M. Vassalloc, and H. Bouchachia, "Smart-cover: A real-time sitting pos-ture monitoring system," *Sensors and Actuators A: Physical*, vol. 317, pp. 112451, 2021, doi:10.1016/j.sna.2020.112451

[13] K. Bourahmoune, K. Ishac, and T. Amagasa, "Intelligent posture training: machine-learning-powered human sitting posture recognition based on a pressure-sensing IoT cushion," *Sensors*, vol. 22, no. 14, pp. 5337, 2022, doi:10.3390/s22145337

[14] J. Roh, H. Park, K. J. Lee, J. Hyeong, S. Kim and B. Lee, "Sitting posture monitoring system based on a low-cost load cell using machine learning," *Sensors*, vol. 18, no. 1, pp. 208, 2018, doi:10.3390/s18010208

[15] H. Jeong and W. Park, "Developing and evaluating a mixed sensor smart chair system for real-time posture classification: Combining pressure and distance sensors," *IEEE Journal of Biomedical and Health Informatics*, vol. 25, pp. 1805-1813, 2020, doi:10.1109/JBHI.2020.3030096

[16] L. M. Ang, K. P. Seng, and M. Wachowicz, "Embedded intelligence and the data-driven future of application-specific internet of things for smart environments," *International Journal of Distributed Sensor Networks*, vol. 18, no. 6, pp. 15501329221102371, 2022, doi:10.1177/15501329221102371

[17] J. Wang, B. Hafidh, H. Dong, and A. El Saddik, "Sitting posture recognition using a spiking neural network," *IEEE Sensors Journal*, vol. 21, no. 2, pp. 1779-1786, 2020, doi:10.1109/JSEN.2020.3016611

[18] F. Luna-Perejón, J. M. Montes-Sánchez, L. Durán-López, A. Vazquez-Baeza, I. Beasley-Bohórquez, and J. L. Sevillano-Ramos, "IoT device for sitting posture classification using artificial neural networks," *Electronics*, vol. 10, no. 15, pp. 1825, 2021, doi:10.3390/electronics10151825

[19] A. Wang, S. Zhao, C. Zheng, H. Chen, L. Liu, and G. Chen, "HierHAR: Sensor-based data-driven hierarchical human activity recognition," *IEEE Sensors Journal*, vol. 21, no. 3, pp. 3353-3365, 2021, doi:10.1109/JSEN.2020.3023860

[20] S. Pan and Q. Yang, "A survey on transfer learning," *IEEE Transactions on Knowledge and Data Engineering*, vol. 22, no. 10, pp. 1345-1359, 2010, doi:10.1109/TKDE.2009.191

Received 26 September 2023